Ocean Sci. Discuss., 12, 1693–1710, 2015
www.ocean-sci-discuss.net/12/1693/2015/
doi:10.5194/osd-12-1693-2015

Ocean Science
Discussions
Open Access

Responses of atmospheric circulation to sea surface temperature anomalies in the South China Sea

M. Zhou and G. Wang

State Key Laboratory of Satellite Ocean Environment Dynamics, Second Institute of Oceanography, State Oceanic Administration, Hangzhou 310012, China

Received: 23 June 2015 – Accepted: 13 July 2015 – Published: 5 August 2015

Correspondence to: G. Wang (gwang@sio.org.cn)

Published by Copernicus Publications on behalf of the European Geosciences Union.

Abstract

The sea surface temperature (SST) anomalies in the South China Sea (SCS) and their influences on global atmospheric circulation were studied. The results of the simple atmospheric model suggested that the SCS SST anomalies can induce several barotropic wave trains from the SCS to other regions such as North America, high latitudes of the Southern Hemisphere and the Mediterranean. The baroclinic stream function anomalies from the simple model showed an anticyclonic vortex pair in East Asia and southern tropical Indian Ocean and a cyclonic vortex pair in the North Pacific and the Southwest Pacific. It is suggested that the spatial pattern of SST anomalies in the SCS can affect the magnitude of stream function anomalies, although it cannot affect the spatial pattern of atmospheric circulation.

1 Introduction

The South China Sea (SCS, 0–25° N, 100–125° E) is the largest marginal sea in the Northwest Pacific. The sea surface temperature (SST) in the SCS has a significant seasonal cycle. The climatological SSTs in summer (June to August) and winter (December to February) over the SCS are shown in Fig. 1. The SST in summer is mostly above 28 °C, with a pronounced cold tongue veering off central Vietnam (Fig. 1a). During winter, the SST is cold in the northwest and warm in the southeast of the SCS (Fig. 1b).

The SST in the SCS had a robust warming trend during past several decades (Luo et al., 1986; Fang et al., 2006; Xie et al., 2010; Zhang et al., 2010; Liu and Zhang, 2013). Based on the Optimum Interpolation Sea Surface Temperature (OISST) dataset, Fang et al. (2006) concluded that the SST in the SCS had the positive linear trend of 5 °C 100 a^{-1} during 1993–2003. The summer and winter SST trends in the SCS from 1982 to 2011 are also shown in Fig. 1. Whether in summer or in winter, the SCS warming trend is significant; with 1.64 °C 100 a^{-1} in summer and 2.04 °C 100 a^{-1} in winter,

OSD
12, 1693–1710, 2015

respectively. The maximum SST trend can exceed 9.50 °C 100 a^{-1}. The averaged SST trend of the SCS is smaller than that reported by Fang et al. (2006), which used the data from 1993–2003. During summer, the larger warming is in the western SCS and the smaller in the eastern SCS. During winter, the larger warming is in the eastern SCS and the smaller in the western SCS.

Many studies focused on the effects of the positive SST anomalies in the SCS on precipitation and climate in China (Zhang et al., 2003; Fong et al., 2004; Roxy and Tanimoto, 2012). According to Zhang et al. (2003), the positive SST anomaly in the SCS in summer was followed by anomalous southward wind, and then more moisture was transferred to South China, which resulted in floods in the Yangtze River Valley. Fong et al. (2004) suggested that the SCS surface warming can enhance latent and sensible heat fluxes from the sea surface and result in a cyclonic circulation anomaly in the lower troposphere and an anti-cyclonic circulation anomaly in the upper troposphere, which then affect the climate of South China. Roxy and Tanimoto (2012) pointed out that the positive SST anomalies over the SCS tended to form a favorable condition for convective activity and enhanced the northward propagating precipitation anomalies during the SCS summer monsoon. Other studies showed that the SST anomalies in the SCS can influence SCS monsoon onset (Johnson and Ciesielski, 2002; Ding et al., 2004; Lestari and Iwasaki, 2006) and its variability (Liu and Xie, 1999; Lestari et al., 2011; Roxy and Tanimoto, 2012).

Previous studies mostly discussed how the SST in the SCS affected the local climate. But the extent of impact of the SST anomalies in the SCS is still not known. In this paper, we use a simple atmospheric model to discuss it. The rest of this paper is organized as follows. Section 2 describes the data and model used in this study. The results obtained with the simple atmospheric model are presented in Sect. 3. Summary and discussion are provided in Sect. 4.

OSD
12, 1693–1710, 2015

2 Data and model

2.1 Data and method

Two datasets are used in this study. The climatological stream functions are from the National Centers for Environmental Prediction/National Center for Atmospheric Research (NECP/NCAR) reanalysis, which is available on a 2.5° latitude by 2.5° longitude grid (Kalnay et al., 1996). OISST analysis product is from the National Oceanic and Atmospheric Administration (NOAA), which has the spatial resolution of 0.25° latitude by 0.25° longitude (Renolds et al., 2002). The period of the two datasets used is from 1982 to 2011.

The basic mean flows are represented by the stream functions at 250 and 750 hPa from the monthly NCEP/NCAR reanalysis. The stream functions at 750 hPa are constructed by linear interpolation with all standard pressure levels, as 750 hPa is not a standard pressure level. Since the model atmosphere is simplified to two levels (centered at 250 and 750 hPa), the stream functions can be separated into the barotropic and baroclinic components as follows:

$$\psi_{\text{barotropic}} = 0.5 \cdot (\psi_{250\,\text{hPa}} + \psi_{750\,\text{hPa}}), \quad (1)$$

$$\psi_{\text{baroclinic}} = 0.5 \cdot (\psi_{250\,\text{hPa}} - \psi_{750\,\text{hPa}}), \quad (2)$$

where ψ stands for stream function.

Figure 2 shows the spatial pattern of mean barotropic stream function (a) and baroclinic stream function (b) from 1982 to 2011. Whether barotropic or baroclinic stream function, it was always the westerly in high latitudes. Generally, there were two westerly jet cores in the Northern Hemisphere and consistent westerly in the Southern Hemisphere. In the equatorial and tropical regions, the flows fluctuated due to strong convections.

OSD
12, 1693–1710, 2015

2.2 Atmospheric model

We use a simple atmospheric model developed recently by Lee et al. (2009) to simulate global atmospheric circulation. This is a steady-state two-level (centered at 250 and 750 hPa) spherical-coordinate primitive equation model, linearized about prescribed background mean flows. The model uses triangular 18 truncations for horizontal grids. The formulation is similar to that of the multi-level linear baroclinic model used by Hoskins and Simmons (1975) and others, but its governing equations are greatly simplified by employing Gill's (1980) simple thermodynamic equation. Detailed description of the simple model can be found in the paper of Lee et al. (2009). This model successfully simulated the local and remote responses of the atmosphere to tropical heating anomalies (Lee et al., 2009; Wang et al., 2010; Zheng et al., 2013). In this study, we use the basic mean flows as the initial conditions and heating in the SCS as the forcing conditions to run this model.

3 Results

3.1 Influence of SST anomalies in the meridional direction

Two experiments are set up to see how basin-scale SST anomalies affect the atmospheric circulation: (1) uniform heating in the SCS (Case 1) and (2) heating decreased northward in the SCS to consider the differences in solar radiation in the northern and southern SCS (Case 2). To test the effects of seasonal SST anomalies in the SCS, we set up two more experiments: (3) heating pattern similar to the SST winter pattern (Case 3) and (4) heating pattern similar to the SST summer pattern (Case 4) in the SCS. As shown in Fig. 1, the SST in the winter is low in the northwest and high in the southeast SCS, which is used in Case 3, while the summer pronounced cold tongue veering off central Vietnam is included in Case 4. Heating patterns derived from SST anomalies for these four experiments are summarized in Fig. 3. The calculations are

OSD
12, 1693–1710, 2015

listed in Table 1. Note the total heat input is the same for the four experiments to ensure comparability.

Figure 4a shows the barotropic stream function anomalies from Case 1. There are three robust waves in the barotropic stream function. The first one is from the SCS to North America through the northwestern Pacific, which is somewhat similar to the classical PNA pattern (Wallace and Gutzler, 1981; Nitta, 1986; Huang, 1984). The second one is from the SCS to high latitudes of the Southern Hemisphere cross the equator. As shown by Wang et al. (2010), the background vertical wind shear is important in converting energy from the heating-induced baroclinic flow anomalies into barotropic motions near the heating source. The barotropic anomalies in turn interact with the mean westerly wind to transmit the barotropic signals to the high latitudes of the Southern Hemisphere. Note another small wave train is from the SCS to the Mediterranean. According to the classical theory of energy dispersion (Yeh, 1949) and the great circle theory (Hoskins and Karoly, 1981), disturbances produced by local heating can spread westward.

The baroclinic stream function anomalies from the simple model show an anticyclonic vortex pair in East Asia and southern tropic Indian Ocean (Fig. 4b). Accordingly, a cyclonic vortex pair appears in the north and southwest Pacific, quite similar to the Matsuno–Gill model (Gill, 1980) and consistent with the results of Heckley and Gill (1984) and Smagorinsky (1953). The response of atmospheric circulation to the heating anomaly in the SCS suggests that the Gill dynamics is at work.

The barotropic and baroclinic stream function anomalies for Cases 2–4 are basically the same as for Case 1, which indicates that the positive heating anomalies in the SCS can all induce three waves in the barotropic stream function and two vortex pairs in the baroclinic stream function regardless of the spatial pattern of the heating. The amplitudes are slightly different in the four experiments. For the PNA-like pattern wave train and the Southern Hemisphere wave train, the barotropic stream functions in Cases 1 and 4 are weaker than those in Cases 2 and 3 in the anticyclonic anomalies, but they are stronger than those in Cases 2 and 3 in the cyclonic anomalies (Fig. 5a).

OSD
12, 1693–1710, 2015

Conversely, the baroclinic stream functions of Cases 1 and 4 are weaker than those in Cases 2 and 3 in the cyclonic anomalies, but are stronger than those in Cases 2 and 3 in the anticyclonic anomalies (Fig. 5b). The differences among the four cases suggest that the spatial pattern of SST anomalies can affect the magnitude of stream functions, although it cannot affect the spatial pattern of atmospheric circulation. The results support that the waves $n = 1, 2$ are distinctly controlled by the asymmetric heating sources revealed by Fu et al. (1980).

3.2 Influence of SST anomalies in the zonal direction

To test the effects of the SST warming patterns in the SCS on atmospheric circulation in the zonal direction, we carry out two more experiments, using summer and winter SST warming trend heating patterns, respectively. Figure 6 shows the stream function anomalies of the barotropic and baroclinic components for Cases 5 and 6, which are also summarized in Table 1. Note the heating pattern in the two experiments is similar to the warming trend pattern, while the total heat input in these two cases is the same as in Cases 1–4 to ensure comparability.

The spatial patterns of the stream function anomalies for Cases 5 and 6 are also quite similar to those in Case 1 for both barotropic or baroclinic components. For the PNA-like pattern wave train or the Southern Hemisphere wave train, the barotropic stream function in Case 5 is weaker than that in Case 6 in the cyclonic anomalies, but is stronger than that in Case 6 in the anticyclonic anomalies (Fig. 6a). Conversely, the baroclinic stream function in Case 5 is weaker than that in Case 6 in the anticyclonic anomalies, but is stronger than that in Case 6 in the cyclonic anomalies (Fig. 6b). As shown in Fig. 1, the larger warming trend is in the western SCS for the summer but in the eastern SCS for the winter. The difference between Cases 5 and 6 suggests that the larger warming trend in the western (eastern) SCS heating pattern can weaken (strengthen) the cyclonic anomalies and strengthen (weaken) the anticyclonic anomalies in the barotropic component. On the contrary, the larger warming trend in the western (eastern) SCS heating pattern can strengthen (weaken) cyclonic anoma-

OSD
12, 1693–1710, 2015

lies and weaken (strengthen) the anticyclonic anomalies in the baroclinic component. It also suggests that the spatial pattern of SST trend can affect the magnitude of stream functions, although it cannot affect the spatial pattern of atmospheric circulation.

4 Summary and discussion

In this study, the influences of SST anomalies in the SCS on global atmospheric circulation were studied. The results of the simple atmospheric model suggested that the SCS heating can induce a barotropic wave train from the SCS to the Northwest Pacific and North America, which is somewhat similar to the classical PNA pattern. Simultaneously, the SCS heating can induce a barotropic wave train from the SCS to high latitudes of the Southern Hemisphere. In particular, we noticed a weak barotropic wave train from the western SCS to the Mediterranean. The baroclinic stream function anomalies from the simple model showed an anticyclonic vortex pair in East Asia and the southern tropic Indian Ocean and a cyclonic vortex pair in the North Pacific and the Southwest Pacific. The stream function anomalies of the barotropic and baroclinic components for all six cases are basically the same, with slight differences in amplitude. It suggests that the spatial pattern of heating can cause some differences in magnitude, but not in circulation patterns. Our findings in this study may be important for the regional and global climate research. For example, we may forecast climate-related events based on the SCS SST anomalies.

Note heating in the atmosphere is not necessarily collocated to SST warming in observations. In some cases, the SST warming results from descending in the atmosphere and thus it may not be a cause of heating. For example, He and Wu (2013) indicated that the SST anomalies in the South China Sea are mostly response to the atmospheric changes except for boreal winter in the northern South China Sea. We completely ignore the situation and simply consider that the SST anomalies can induce heat to the atmosphere. Thus a more complete atmospheric general circulation model is necessary to confirm these findings.

OSD
12, 1693–1710, 2015

Acknowledgements. We thank Sang-Ki Lee and Chunzai Wang for sharing the model code and helping to run the model. This study was supported by the National Basic Research Program of China and the National Natural Science Foundation of China.

References

Ding, Y. H., Li, C. Y., and Liu, Y. J.: Overview of the South China Sea monsoon experiment, Adv. Atmos. Sci., 21, 343–360, doi:10.1007/BF02915563, 2004.

Fang, G., Wei, H., Chen, Z., Wang, Y., Wang, X., and Li, C.: Trends and interannual variability of the South China Sea surface winds, surface height, and surface temperature in the recent decade, J. Geophys. Res., 111, C11S16, doi:10.1029/2005JC003276, 2006.

Fong, S. K., Wu, C. S., Wang, A. Y., Ku, C. M., Hao, I. P., and Tong, T. N.: A numerical study of the effects of South China Sea SST anomalies on the climate in South China, J. Trop. Meteorol., 20, 32–38, 2004 (in Chinese).

Fu, K. Z., Wu, H. D., Fang, X. F., and Wang, Y. K.: Asymmetric heating effects on the general circulation of atmosphere, Acta Meteorol. Sin., 38, 205–218, 1980 (in Chinese).

Gill, A. E.: Some simple solutions for heat-induced tropical circulation, Q. J. Roy. Meteorol. Soc., 106, 447–462, doi:10.1002/qj.49710644905, 1980.

He, Z. Q. and Wu, R. G.: Seasonality of interannual atmosphere–ocean interaction in the South China Sea, J. Oceanogr., 69, 699–712, doi:10.1007/s10872-013-0201-9, 2013.

Heckley, W. A. and Gill, A. E.: Some simple analytical solutions to the problem of forced equatorial long waves, Q. J. Roy. Meteorol. Soc., 110, 203–217, doi:10.1002/qj.49711046314, 1984

Hoskins, B. J. and Karoly, D. J.: The steady linear response of a spherical atmosphere to thermal and orographic forcing, J. Atmos. Sci., 38, 1179–1196, doi:10.1175/1520-0469(1981)038<1179:TSLROA>2.0.CO;2, 1981.

Hoskins, B. J. and Simmons, A. J.: A multi-layer spectral model and the semi-implicit method, Q. J. Roy. Meteorol. Soc., 101, 637–655, doi:10.1002/qj.49710142918, 1975.

Huang, R. H.: The characteristics of the forced stationary planetary wave propagations in summer Northern Hemisphere, Adv. Atmos. Sci., 1, 84–94, doi:10.1007/BF03187619, 1984.

OSD

12, 1693–1710, 2015

Johnson, R. H. and Ciesielski, P. E.: Characteristics of the 1998 summer monsoon onset over the northern South China Sea, J. Meteorol. Soc. Jpn. Ser. II, 80, 561–578, doi:10.2151/jmsj.80.561, 2002.

Kalnay, E., Kanamitsu, M., Kistler, R., Collins, W., Deaven, D., Gandin, L., Iredell, M., Saha, S., White, G., Woollen, J., Zhu, Y., Leetmaa, A., Reynolds, B., Chelliah, M., Ebisuzaki, W., Higgins, W., Janowiak, J., Mo, K. C., Ropelewski, C., Wang, J., Jenne, R., and Joseph, D.: The NCEP/NCAR 40-year reanalysis project, B. Am. Meteorol. Soc., 77, 437–471, doi:10.1175/1520-0477(1996)077<0437:TNYRP>2.0.CO;2, 1996.

Lee, S. K., Wang, C. Z., Mapes, B. E.: A simple atmospheric model of the local and teleconnection responses to tropical heating anomalies, J. Climate, 22, 272–284, doi:10.1175/2008JCLI2303.1, 2009.

Lestari, R. K. and Iwasaki, T.: A GCM study on the roles of the seasonal marches of the SST and land–sea thermal contrast in the onset of the Asian summer monsoon, J. Meteorol. Soc. Jpn. Ser. II, 84, 69–83, 2006.

Lestari, R. K., Watanabe, M., and Kimoto, M.: Role of air–sea coupling in the interannual variability of the South China Sea summer monsoon, J. Meteorol. Soc. Jpn. Ser. II, 89, 283–290, doi:10.2151/jmsj.2011-A18, 2011.

Liu, Q. and Zhang, Q.: Analysis on long-term change of sea surface temperature in the China Seas, J. Ocean Univ. China, 12, 295–300, doi:10.1007/s11802-013-2172-2, 2013.

Liu, W. T. and Xie, X.: Space-based observations of the seasonal changes of South Asian monsoons and oceanic response, Geophys. Res. Lett., 26, 1473–1476, doi:10.1029/2003JC001867, 1999.

Luo, S. H. and Jin, Z. H.: Statistical analyses for sea surface temperature over the South China Sea, behavior of subtropical high over the west pacific and monthly mean rainfall over the Chang Jiang middle and lower reaches, J. Atmos. Sci., 10, 409–418, 2006 (in Chinese).

Nitta, T.: Long-term variations of cloud amount in the western Pacific region, J. Meteorol. Soc. Jpn., 64, 373–390, 1986.

Reynolds, R. W., Rayner, N. A., Smith, T. M., Stokes, D. C., and Wang, W. Q.: An improved in situ and satellite SST analysis for climate, J. Climate, 15, 1609–1625, doi:10.1175/1520-0442(2002)015<1609:AIISAS>2.0.CO;2, 2002.

Roxy, M. and Tanimoto, Y.: Influence of sea surface temperature on the intraseasonal variability of the South China Sea summer monsoon, Clim. Dynam., 39, 1209–1218, doi:10.1007/s00382-011-1118-x, 2012.

OSD
12, 1693–1710, 2015

Smagorinsky, J.: The dynamical influence of large-scale heat sources and sinks on the quasi-stationary mean motions of the atmosphere, Q. J. Roy. Meteor. Soc., 79, 342–366, doi:10.1002/qj.49707934103, 1953.

Wallace, J. M. and Gutzler, D. S.: Teleconnections in the geopotential height field during the Northern Hemisphere winter, Mon. Weather Rev., 109, 784–812, doi:10.1175/1520-0493(1981)109<0784:TITGHF>2.0.CO;2, 1981.

Wang, C. Z., Lee, S. K., and Mechoso, C. R.: Interhemispheric influence of the Atlantic warm pool on the southeastern Pacific, J. Climate, 23, 404–418, doi:10.1175/2009JCLI3127.1, 2010.

Xie, S. P., Deser, C., Vecchi, A. G., Ma, J., Tend, H., and Wittenberg, A. T.: Global warming pattern formation: sea surface temperature and rainfall, J. Climate, 23, 966–986, doi:10.1175/2009JCLI3329.1, 2010.

Yeh, T.: On energy dispersion in the atmosphere, J. Meteorol., 6, 1–16, doi:10.1175/1520-0469(1949)006<0001:OEDITA>2.0.CO;2, 1949.

Zhang, Q., Liu, P., and Wu, G. X.: The relationship between the flood and drought over the lower reach of the Yangtze River Valley and the SST over the Indian Ocean and the South China Sea, J. Atmos. Sci., 27, 992–1006, 2003 (in Chinese).

Zhang, L. P., Wu, L. X., Lin, X. P., and Wu, D. X.: Modes and mechanisms of sea surface temperature low-frequency variations over the coastal China seas, J. Geophys. Res., 115, C08031, doi:10.1029/2009JC006025, 2010.

Zheng, J., Liu, Q. Y., Wang, C. Z., and Zheng, X. T.: Impact of heating anomalies associated with rainfall variations over the indo-western Pacific on Asian atmospheric circulation in winter, Clim. Dynam., 40, 2023–2033, doi:10.1007/s00382-012-1478-x, 2013.

OSD
12, 1693–1710, 2015

Table 1. The heat forcing Q at each grid for Cases 1–6.

Exp.	Heat forcing in the SCS	Description
Case 1	$Q(i,j) = Q_0$ *	uniform heating
Case 2	$Q(i,j) = Q_0 \cdot (25 - \mathrm{lat}(i,j))/12.5$	heating less in the north
Case 3	$Q(i,j) = Q_0 \cdot ((25 - \mathrm{lat}(i,j)) + (125 - \mathrm{lon}(i,j)))/25$	similar to SST winter pattern
Case 4	$Q(i,j) = Q_0 \cdot ((12.5 - \mathrm{lat}(i,j))^2/10 + \mathrm{lon}(i,j) - 100)/18.125$	similar to SST summer pattern
Case 5	$Q(i,j) = Q_0 \cdot$ summer SST trends pattern$/1.64$	summer SST trends pattern
Case 6	$Q(i,j) = Q_0 \cdot$ winter SST trends pattern$/2.04$	winter SST trends pattern

* $Q_0 = 1.16 \times 10^{-2}\,\mathrm{W\,kg^{-1}}$ ($1\,^{\circ}\mathrm{C\,day^{-1}}$).

OSD
12, 1693–1710, 2015

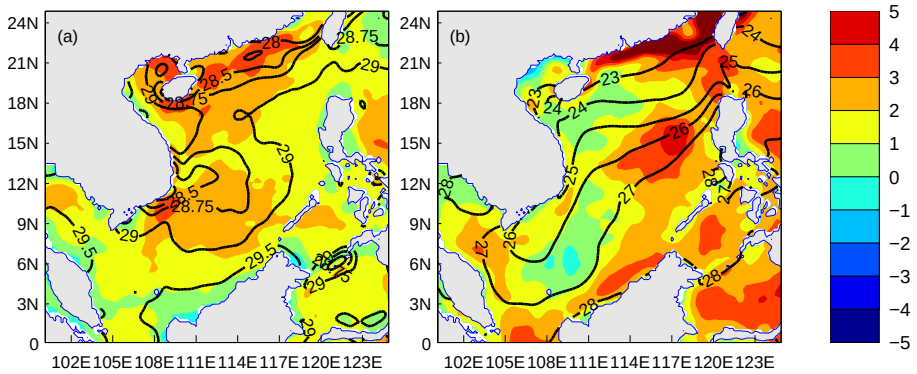

Figure 1. (a) Summer- and **(b)** winter-mean SST (contours; units: ˚C) and SST trends (color shading; units: ˚C 100 a^{-1}) in the SCS from 1982 to 2011.

OSD
12, 1693–1710, 2015

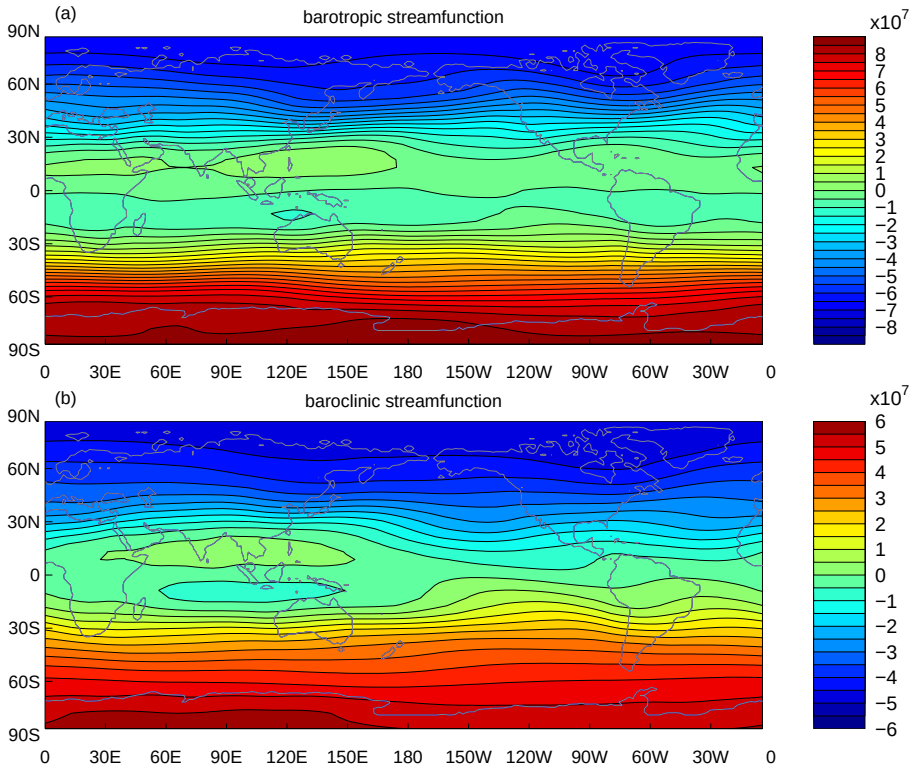

Figure 2. (a) Barotropic and **(b)** baroclinic stream functions in climatology. The contour interval is $5.0 \times 10^6\ m^2\ s^{-1}$.

OSD
12, 1693–1710, 2015

Responses to SST anomalies in South China Sea

M. Zhou and G. Wang

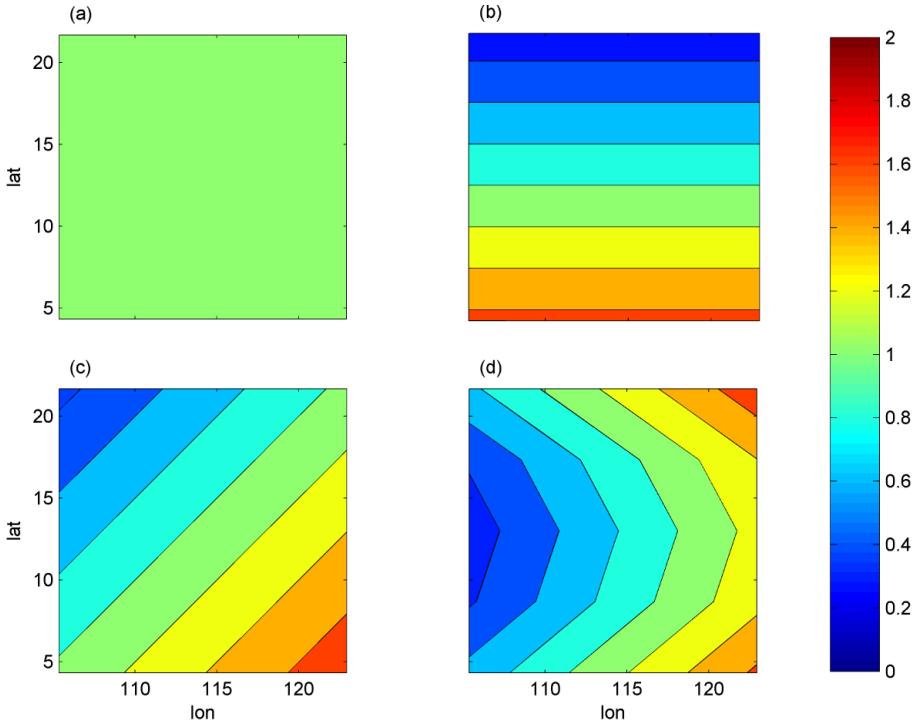

Figure 3. Spatial patterns of heat forcing Q for case 1–4 (**a–d**, units: Q_0).

OSD
12, 1693–1710, 2015

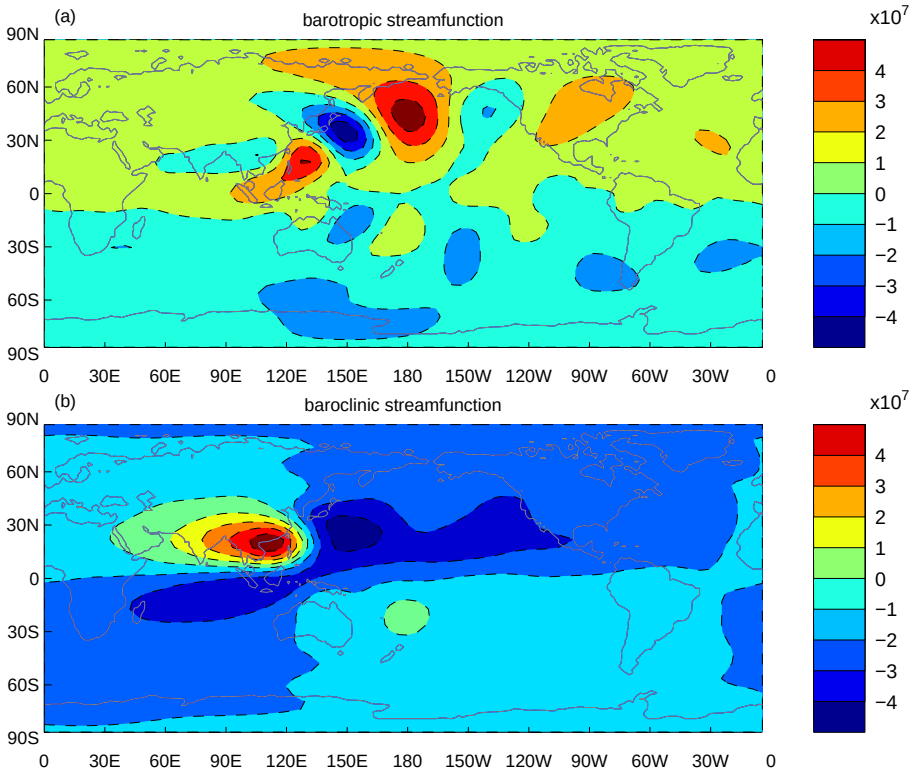

Figure 4. Barotropic **(a)** and baroclinic **(b)** stream function anomalies for Case 1. The contour interval is $1 \times 10^6\ m^2\ s^{-1}$.

OSD
12, 1693–1710, 2015

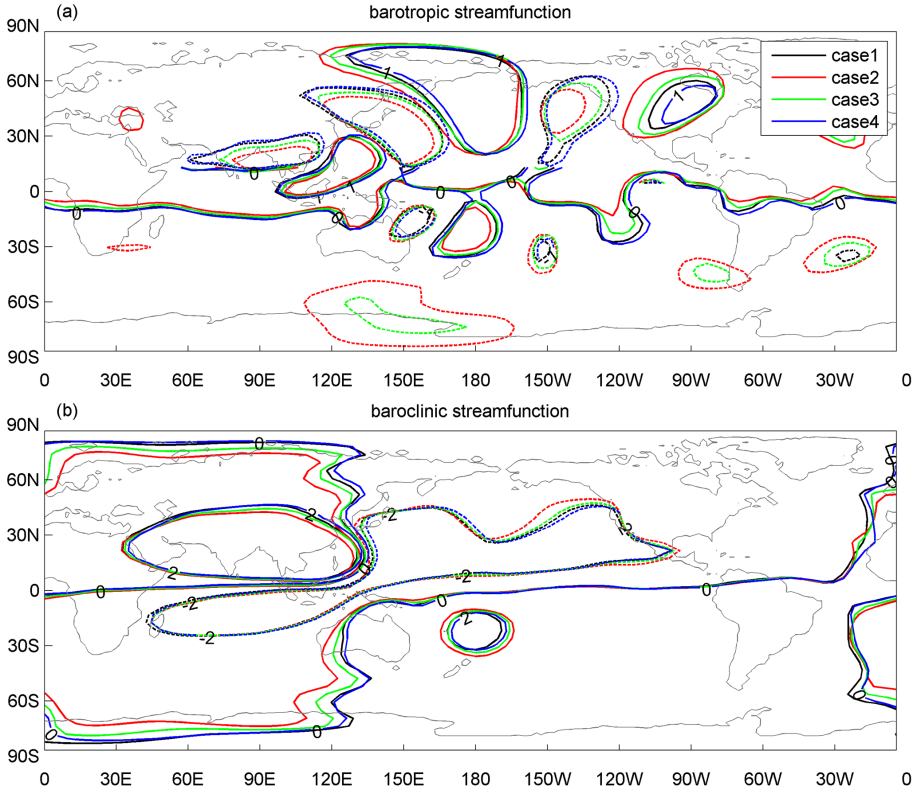

Figure 5. (a) Barotropic and **(b)** baroclinic stream function anomalies (units: $10^6\,m^2\,s^{-1}$) for Cases 1–4 (the black, red, green, and blue contours are stream function anomalies for Cases 1, 2, 3, and 4, respectively). The contour interval is $2 \times 10^6\,m^2\,s^{-1}$.

OSD
12, 1693–1710, 2015

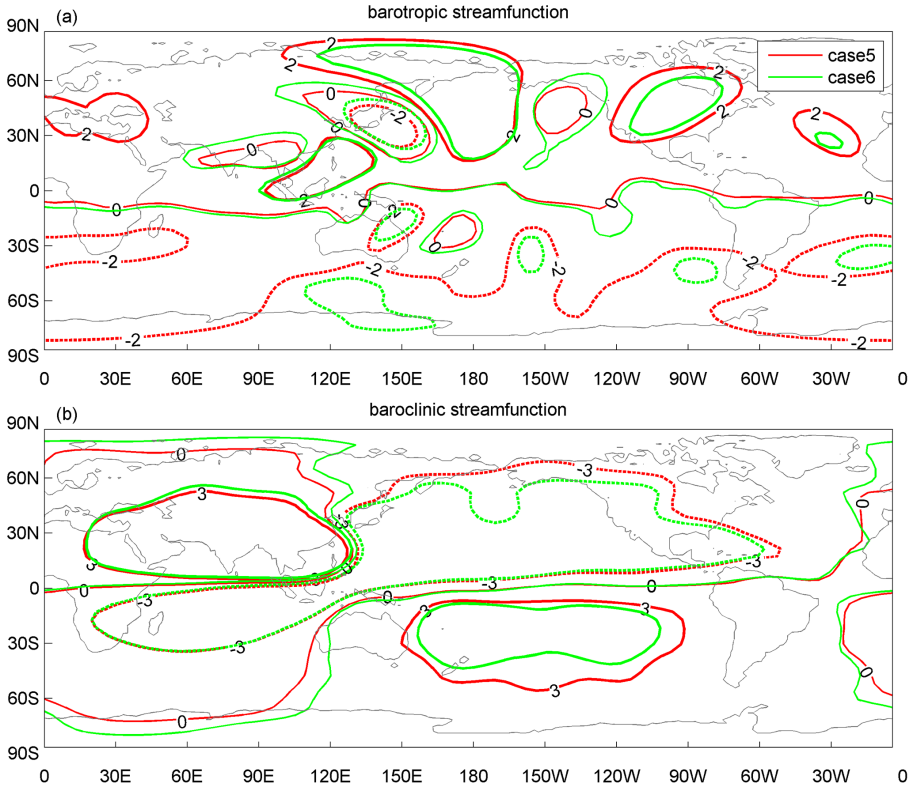

Figure 6. (a) Barotropic and **(b)** baroclinic stream function anomalies ($10^6\,m^2\,s^{-1}$) for Cases 5 (red contours) and 6 (green contours). The contour interval is $2 \times 10^6\,m^2\,s^{-1}$ in the top panel and $3 \times 10^6\,m^2\,s^{-1}$ in the bottom panel.

OSD
12, 1693–1710, 2015